Contribution to photon isolation performance in ATLAS

Dafne Arias. *Université Paris VII*

29/03/2016

The context of photon production in hadronic colliders is presented. The internship plan within the ATLAS group in the LPNHE is provided. The criteria for isolated photons used in Tevatron, ATLAS and CMS as well as the theoretical definitions are discussed.

1 Introduction

The standard model (SM) describes the relationship between the known fundamental interactions and the elementary particles that make up all matter, summarizing the actual knowledge in particle physics. Almost all the experimental tests of the forces described by the SM agree with their predictions. However, it leaves many unsolved questions. The use of particle colliders has played an important role in studying the SM. One of these colliders is the LHC, the largest machine ever built. The (**L**arge **H**adron **C**ollider) is a particle accelerator and collider located at CERN designed for the collision of hadrons at a center-of-mass energy of 14 TeV. It is composed by different experiments, whose four major ones are ATLAS, CMS, ALICE and LHCb.

The measurements at the LHC related with the production of prompt photons (which do not come from hadron decays) provide an unique framework to test the predictions of QCD. In addition, these kind of processes are background sources for several electroweak physics, Higgs physics and in searches for physics beyond the standard model.

This written synopsis presents the experimental criteria of photon isolation used in physics experiments, as a technique for the identification of prompt photons.

In Section. 2 a summary of the work proposed for the internship is given. In Section. 3 the experimental tools for test photon production is introduced briefly. In Section. 4 the isolation criteria used in Tevatron, ATLAS and CMS experiments are presented following the results of their respective collaborations. In Section. 5 the final summary of the synopsis and the future prospects of the internship is given.

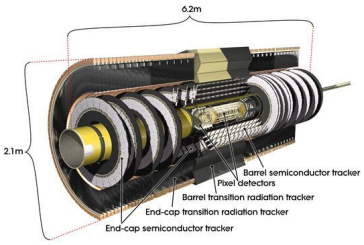

Figure 1: *ATLAS Inner Detector (ID), measures the direction, momentum, and charge of electrically-charged particles produced in each proton-proton collision.*

1.1 ATLAS detector

The ATLAS (**A** **T**orodial **L**HC **A**pparatu**S**) detector is one of the multipurpose experiments in the LHC designed for the study of proton-proton collisions. ATLAS has a symmetric cylindrical geometry (46m long, 25m in diameter, and sits 100m below ground) and it is composed by 6 sub-detectors wrapped concentrically in layers around the collision point to record the trajectory, momentum, and energy of particles. ATLAS has two magnet systems for bending the paths of the charged particles: a solenoid around the ID (inner detector), and a toroid in the most external layer.

The major components of the ATLAS detector are the Inner Detector (Figure. 1), the Calorimeters (Figure. 2) and the Muon Spectrometer.

The most relevant sub-detector for this internship is the LAr (Liquid Argon calorimeter).

1.2 Scientific Goal

Precision performance of photon reconstruction in hadron colliders are useful for a variety of topics:

1 Detailed understanding of the underlying parton picture.

2 The measurement of the production cross section of a single-photon or photon pairs not originating from hadronic decays, provides a tool to probe perturbative

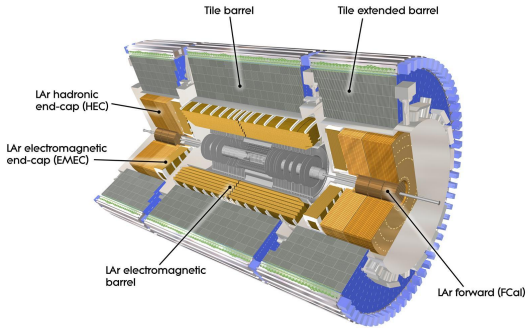

Figure 2: *ATLAS calorimeter system.*

QCD since they emerge without the hadronization phase.

3 It is an important signal component in several SM, Higgs and BSM studies and also requires an efficient background rejection.

1.3 Presentation of the Lab.

The intership will be performed at the Laboratoire de Physique Nuclaire et de Hautes Energies (LPNHE - Paris) in the ATLAS group, under the supervision of José Ocariz.

LPNHE consists of 12 research groups. The laboratory is involved in several experimental programs in the framework of international collaborations with very large research infrastructures. These programs cover current issues in particle physics, astroparticle and cosmology.

The LPNHE Atlas group consists of 28 researchers and has been strongly involved (among many other subjects) in the LAr (**L**iquid **Ar**gon calorimeter) construction and the identification and measurement of the photons and electrons in this detector, due to the crucial role that it plays in photons physics and, for example, the decay of Higgs in two photons, and many important physics processes at the LHC.

It participated in the construction and start up of the electromagnetic calorimeter (which has been the historical activity of the group). Also, the group has participated in the construction of the inner layer for the pixel detector installed for Run2 in 2015.

The group is involved in the activities for upgrading the internal detector for the phase of hight luminosity (sLHC) as also the development of the scientific computing required to process the data produced by the collisions. Among other topics in which the group is involved there are, the study of the top quark, the Higgs and in general, precision measurements in the standard model of particle physics and the new physics beyond this model.

Group members are actively participating in the analysis of BSM physics with photons, including the search and study of resonance in diphoton spectrum at high mass, in data recorded in 2015 at 13 TeV there is an excess of 3.6 sigma bump at 750 GeV.

Within this group there are 18 complete PhD theses and 8 theses are currently underway.

2 Summary of the intership project and schedule

The internship at LPNHE will last 14 weeks and the specific topic is photon isolation. In the first two weeks a bibliographic report of the subject and the phenomenology of photon production in QCD will be made. After that, the main activity will be a contribution to the performance studies about the optimization of the photon isolation criteria with the ATLAS detector at LHC.

On the first part of the internship, an analysis of the data from the Run 2 recorded in 2015 at 13 TeV will be perform using ROOT/C++ and multivariable methods for the statistical analysis. The agreement between the ATLAS data and the simulation will be assessed, and the efficiencies and purities of single isolated photons will be estimated. For the second part of the internship (only if possible), an analysis of the new data coming in spring 2016 is going to be made with the same methods.

As part of other competences targeted by the internship, it can be mentioned the work within a large international collaboration and the participation in the meetings of the "photon" sub-group in the LPNHE.

3 Status of the field

Since the decade of 1970 numerous experimental and theoretical efforts and contributions have been made in the production of direct photons in hadronic collisions. In the next table is presented the variety of experiment since 1976 till 2011, in a large range of energies [1].

Experiment	Accelerator	Initial State	$\sqrt{s}$ or E(GeV)	Year
SFM	ISR	pp	45, 53	1976
R108	ISR	pp	62.4	1980
R806	ISR	pp	63	1982
R807	ISR	pp,p$\bar{p}$	53	1985
NA24	SPS f.t.	$\pi^{\pm}$,pp	E = 300	1987
WA70	SPS	pp	280	1988
UA1	Sp$\bar{p}$S	p$\bar{p}$	546, 630	1988
UA2	Sp$\bar{p}$S	p$\bar{p}$	630	1988
R110	ISR	pp	63	1989
UA2	Sp$\bar{p}$S	p$\bar{p}$	630	1992
E706	Fermilab	$\pi-$Be, pBe	E = 500	1992
UA6	SPS	pp,p$\bar{p}$	24.3	1993
E704	Fermilab	p-H liquid	E = 200	1995
CDF	Tevatron	p$\bar{p}$	1800	1995
D0	Tevatron	p$\bar{p}$	1800	1996
UA6	SPS	pp,p$\bar{p}$	24.3	1998
E706	Fermilab	$\pi-$Be(pBe)	E = 515(530, 800)	1998
D0	Tevatron	p$\bar{p}$	1800	2000
D0	Tevatron	p$\bar{p}$	1800, 630	2001
CDF	Tevatron	p$\bar{p}$	1800, 630	2002
CDF	Tevatron	p$\bar{p}$	1800	2004
E706	Fermilab	$\pi-$Be(pBe)	E = 515(530, 800)	2004
PHENIX	RHIC	pp	200	2005
D0	Tevatron	p$\bar{p}$	1960	2006
PHENIX	RHIC	pp	200	2007
CDF	Tevatron	p$\bar{p}$	1960	2009
CMS	LHC	pp	7000	2010
ATLAS	LHC	pp	7000	2011

Table 1: *Chronological summary of measures about direct photon production in different accelerators.*

On the other hand, the study of the diphoton decay channel ($H \longrightarrow \gamma\gamma$) has play an essential part in the discovery of the Higgs boson in 2012 [2] as well in the improvement of this boson signal [3] in recent years.

Useful experimental information can be extracted from photon production data in the hadron colliders. In recent years, Tevatron [6], and also CMS [5] and ATLAS [4] collaborations, have made recent measures of the production cross section of events with isolated photons in the final state and prompt photons, using reconstruction strategies and other approaches. These results have provided tests of perturbative QCD (pQCD) in LO, NLO and NNLO.

4 Discussion

The written synopsis about photon isolation is based on several experimental papers corresponding to different experiments (Tevatron, CMS and ATLAS) plus one theoretical. In this Section. 4, the criteria for photon isolation in recent measurements made at D0+CDF [6] (2009), CMS [5] (2011) and ATLAS [4] (2013) as well the criteria for the identification of photons in ATLAS, is discussed. At the end are presented the results of cross section measurements of photon production in these experiments.

4.1 Definition of isolation

Photons resulting from the hard interaction are usually separated from jets produced in the event, while photons from hadronization and decay processes will always be inside hadronic jets. To disentangle prompt photons from secondary photons, one applies the **isolation technique**, which limits the hadronic activity around a photon candidate, thereby defining an *isolated photon*.

Due to the remaining mixture between processes in the signal, it is important to properly model the variable isolation and its relation to the one used at partonic level in perturbative QCD calculations.

4.1.1 Theoretical

In the case of the theoretical definitions, the reference will be the work of S. Frixione in [7], where the formula for an isolated-photon cross section is defined. This paper constitutes an approach to the subject of isolated photons in pQCD, but at the experimental level, no one has managed to completely implement the "Frixione isolation".

Photons are produced in scattering phenomena by 2 mechanisms:

1. **Direct process**: computable in pQCD. These photons are well isolated from the final state hadrons.

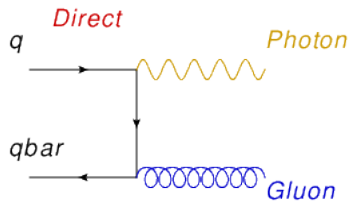

Figure 3: *Feynman diagram example for the direct photon production.*

2. **Fragmentation process**: a QCD parton fragments non-perturbatively into a photon, at a scale of the order of the typical hadronic mass. The unknowns are collected in the quark-to-photon and gluon-to-photon fragmentation functions, so these photons lie inside hadronic jets.

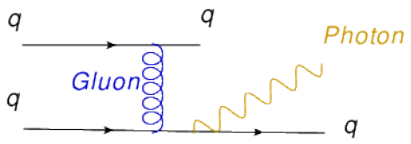

Figure 4: *Feynman diagram example for the fragmentation process.*

But in pQCD, it is not possible to separate sharply the photon from the partons. So 2 methods for resolve this problem are proposed:

1. **Cone approach**: a cone around the photon axis (Figure. 5) is defined; if only a small hadronic energy is found inside the cone, the partons accompanying the photon are clustered with a given jet-finding algorithm (basically the approach that is used in the experimental part).

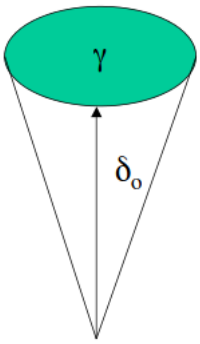

Figure 5: *Cone of angle δ_0 around the photon axis.*

2. **Democratic approach**: the photon is treated as a parton as far as the jet-finding algorithm is concerned. This approach is more suited that the first one to extract the non-perturbative parton-to-photon fragmentation functions from the data. It is a purely collinear phenomenon.

The *cone approach* can be modified in order to get a cross section which only depends upon the *direct process*, and is IR (infra-red) safe at any order in perturbative QCD.

If no parton is found inside a cone around the photon axis, the configurations where the partons are collinear to the photon are rejected, and therefore the contribution of the fragmentation process is exactly zero. But this is not IR safe, because soft gluons can not be emitted inside the cone.

So, to define a IR cross section, there should be no region of forbidden radiation in the phase space, while to eliminate the dependence upon the fragmentation functions such a region must exist. As the fragmentation mechanism is a collinear phenomenon, the contribution to the cross section has to be eliminate making a veto to the collinear configuration only.

In practice, this can be achieved in the following way. A cone around the photon axis of fixed half-angle δ_0 is drawn. Then, for *all* $\delta \leq \delta_0$, the total amount of hadronic energy $E_{tot}(\delta)$ drawn around the photon axis is required to fulfil the following condition:

$$E_{tot}(\delta) \leq \kappa\delta^2. \tag{1}$$

This implies that the energy of a parton emitted exactly collinear to the photon must vanish. This is the basic condition used to reject events.

The cross section of isolated photons plus jets is defined by fixing the parameter δ_0 and applying to each event a procedure called *isolation cuts*:

1 For each set of hadrons i, evaluate the angular distance $R_{i\gamma}$ between i and the photon. In the (η, ϕ) plane:

$$R_{i\gamma} = \sqrt{(\eta_i - \eta_\gamma)^2 + (\varphi_i - \varphi_\gamma)^2}. \tag{2}$$

2 Reject events unless the following condition is fulfilled:

$$\sum_i E_i \theta(\delta - R_{i\gamma}) \leq \chi(\delta), \tag{3}$$

where due to $\theta(\delta - R_{i\gamma})$, the sum gets contribution only from those hadrons whose angular distance from the photon is smaller than or equal to δ. The function χ here, plays the role of $\kappa\delta^2$ in Eq. (1).

The function χ must vanish when its argument tends to zero, $\chi(\delta) \longrightarrow 0$ for $\delta \longrightarrow 0$.

3 Apply a jet-finding algorithm to the hadrons of the event (therefore, the photon is excluded).

4 Apply any other additional cuts to the photon and to the m-candidate jets which lie outside the cone.

An event which is not rejected when the isolation cuts are applied is by definition an **isolated-photon plus m-jet event**. The key point in this procedure is step 2: hadrons are allowed inside the isolation cone. The jets which accompany the photon are the candidate jets outside the isolation cone which also pass the additional cuts. The resulting cross section is therefore totally exclusive in the variables of these jets and of the photon, and inclusive in the variables of the hadrons found inside the isolation cone.

Frixione defines:

$$\chi(\delta) = E_\gamma \epsilon_\gamma \left(\frac{1 - \cos\delta}{1 - \cos\delta_0} \right)^2, \tag{4}$$

where:

$$\lim_{\delta \to 0} \chi(\delta) = 0. \tag{5}$$

Equation (4) implies that, closer to the photon, less hadronic activity is allowed inside the cone, and by that it eliminates all the fragmentation components in an IR safe way.

The main problem with the Frixione isolation criteria is the complication of carrying it out experimentally. As it is explained in [8], this is because of the finite size of the calorimeter cells used to measure the electromagnetic showers. Frixione cone criterion must be applied beyond a minimum distance that depends of the detector in the (η, φ) plane, which kills its continuity property up to r=0. In addition, the transverse energy in the experimental isolation cone is deposited in discrete cells of finite size. Therefore concerning its experimental implementation, the criterion initially proposed by Frixione has to be replaced by a discretized version consisting of a finite number of cones.

4.1.2 Experimental Isolation

From the experimental point of view, it is essential to require the photon to be isolated, and one important issue is to distinguish direct photons (which are produced in the hard processes) from fake photons coming from jets (which are not direct and produced in hadron decays). The challenge is to have a signal without the contamination from the secondary photons are originate in the hadronic decays of mesons like for example π^0, η or ω. The precision criteria differ among experiments, but in general, in all of them the energy deposited in a a cone around the photon is estimated:

$$E_T^{iso} \equiv \sum_i^{cone} E_T^i, \tag{6}$$

where E_T is the transversal energy. The total E_T^i:

$$E_T^{iso} < E_{T,max}^{iso}. \tag{7}$$

Here, the total transversal energy in a cone of radius R centered on the photon in the $\eta\varphi$ plane must be less that a maximum value, define as $E_{T,max}^{iso}$

4.2 Experimental Photon ID in ATLAS

Experimentally, the identification of photons (photon ID) is particularly challenging in hadrons colliders since the overwhelming majority of final state photons originate from neutral hadron decays or from radiative decays of other particles.

In the ATLAS experiment, first, events must pass the three trigger levels and after being accepted, an identification algorithm is applied (for more reference about ATLAS trigger [1]). The photon ID algorithm relies on rectangular cuts using calorimetric variables (these variables describe the shape and structure of electromagnetic showers according to their propagation in the detector, for a detailed description see [9]), defined using energy deposit in the electromagnetic calorimeter cells. The optimal size of the rectangular cuts depend on the type of particle to reconstruct and the region in the calorimeter.

In general the electromagnetic showers by electrons are very similar to the photons, the difference is that they have a track, but for photons, the criteria can be complicated when they convert before reaching the EMC. Then, the ATLAS ID tracking system can reconstruct conversion vertices up to a radius $R < 80cm$ in the transverse plane of the EMC.[1] If there is no trace associated to a given cluster from a rectangular cut, this is classified as a unconverted photon, see Figure. (6). In the other case, the photon candidate is classified as a converted photon.

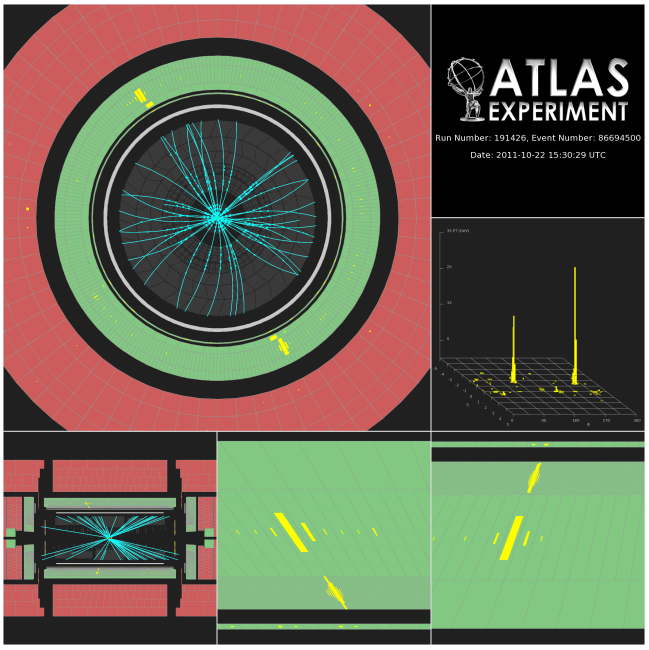

Figure 6: *Event display, the photon in the bottom right is unconverted (no trace associate to the electromagnetic).*

To decide the final classification, additional criteria are applied, and two reference sets of cuts called loose and tight, are defined.[2] The loose selection is mainly used for triggering purposes. The tight selection is separately optimized for unconverted and converted photons to provide a photon identification efficiency of about 85 percent for photon candidates with transverse energy $E_T > 40$GeV.

[1] Only those conversions that occur at a distance $R < 80cm$ are efficiently reconstructed. The probability of conversion varies [1].

[2] The loose criterion favors large efficiency, while the tight criteria favours larger purity.

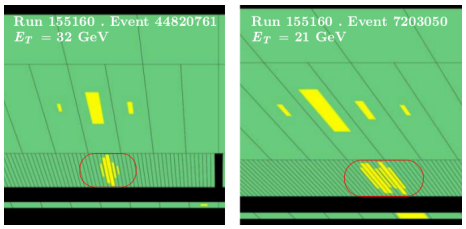

Figure 7: *Energy deposited in the EMC for a photon (left) and a pion decaying in 2 photons (right).*

4.3 Isolation criteria in ATLAS

In this paper [4], the full 2011 data set with a luminosity of $4.9fb^{-1}$ at $\sqrt{s} = 7$TeV is used for the measurement of the total cross section for two isolated photons with $E_T = 25$GeV and $E_T = 22$GeV with and angular separation of $\Delta R > 0.4$.

Historically, ATLAS first used the isolation variable E_T^{40} (for a cone of radius 0.4). For the 2011 LHC data an important pile-up dependence had to be corrected. [3]

So, a new isolation variable was defined [10] with noise correction and pile-up independence called $E_T^{topo,40}$, which improves background rejection and the agreement between the data and the Monte Carlo simulation.

Essentially for E_T^{40} all cells of the cone were being considered, that is, all cells in the calorimeters (the electromagnetic one and the hadronic), see Figure. (8). While for the $E_T^{topo,40}$ only cells belonging to topological clusters (a local maximum with an energy over a threshold) were considered. A representation of topological clusters can be seen in Figure. (9).

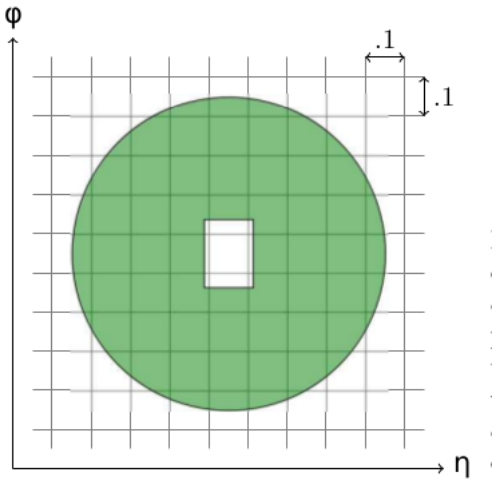

Figure 8: *Cone illustration, this one is on the center of the photon and has a size of $\Delta R = 0.4$. In order to remove the energy of the photon, the cells in the central region are not included using a window but for the rest, all green cell are used.*

[3] Pile-up is the superposition of multiple particle collisions during a bunch crossing. As luminosity increase, so does increases the pile-up. The effects of the pile-up, the calorimeter noise and the hadronization energy tend to increase the isolation energy.

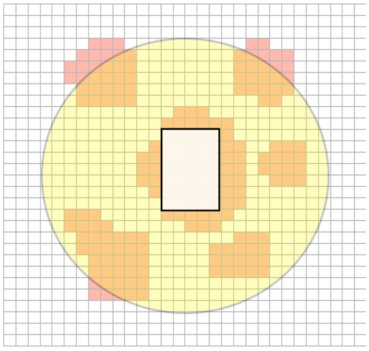

Figure 9: *Sketch of the cone where the energy of the photon is excluded in a window of 5 x 7 rectangle. In the $E_T^{topo,40}$ variable, only the orange cells who represent topological clusters are used.*

Intuitively, the topological argument works better because it is including with the clusters less noise. It was shown that $E_T^{topo,40}$ is much less pile-up dependent that the first variable.

In the first analyses of 2015 data at 13 TeV [11] (for example the search for new resonances in the decay of two photons), an additional isolation criterion was used, based on track isolation. p_T^{iso} is the scalar sum of the p_T of the tracks from the primary vertex with $p_T > 1$GeV in a $\Delta R = 0.2$ cone around each the photon candidate. This improves the efficiency of the isolation selection for events with large pile-up [12].

4.4 Background in ATLAS

The major source of background in these experiments comes from the decays of hadrons and fake photons produced by the fragmentation of partons.

In the case of ATLAS for the measurement of isolated-photon pairs in [4], after the event selection, the jet background is statistically subtracted. The analysis uses the photon $E_T^{topo,iso}$ and the identification criteria simultaneously to discriminate prompt photons from jets. In Figure. 10 is shown the projection of E_T^{iso} of the leading and subleading photon candidates.

4.5 Isolation criteria in CMS

The CMS collaboration reported a measurement of the differential cross section for the inclusive production of isolated prompt photons in the range of $|\eta| < 2.5$ and in the transverse energy range $25 < E_T < 400$GeV.

In CMS criteria the isolation energy are defined separately in tracks (Iso_{TRK}), electromagnetic calorimeter energy (Iso_{ECAL}) and hadron calorimeter (Iso_{HACL}) energy:

- Iso_{TRK}: sum of the transverse momenta p_T of all tracks in a hollow cone $0.04 < R < 0.4$ around the photon direction. The tracks pointing to a rectangular strip of width $|\eta| = 0.015$ centred around the photon position are removed from the sum. The preselection criteria applied to increase the signal fraction of the photon sample (cut) is $Iso_{TRK} < 2.0$GeV.

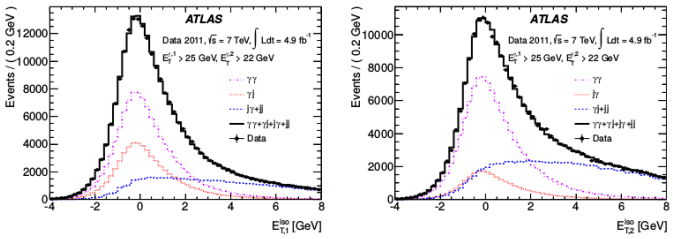

Figure 10: *Shows the projections of two-dimensional fit to the transverse isolation energies of the leading (left) and subleading (right) photon candidates in ATLAS ([4]) (2013). In both figures, the blue dashed represents the background component in the photon candidate's sample: for the leading candidate this is due to jet-gamma and dijet final states, whereas for the sub-leading candidate it comes from gamma-jet and dijet final states.*

- Iso_{ECAL}: the sum the E_T in the individual ECAL crystal located in a hollow cone, with an inner radius of 3.5 crystal and an outer radius of R=0.4, around the ECAL cluster. The photon energy is also substracted from the sum. $Iso_{ECAL} < 4.2$GeV.

- Iso_{HACL}: the sum of E_T in the individual HCAL in a cone $0.15 < R < 0.4$ centred on the ECAL cluster. Must satisfy $Iso_{HCAL} < 2.2$GeV.

In CMS, photon candidates are identified with two complementary methods, one based on photon conversion in the tracker and the other on isolated energy deposits in the electromagnetic calorimeter. Due to the strong magnetic field, the energy deposited in EMC by converted photons is therefore clustered at the electromagnetic calorimeter level by building a cluster that is extended in φ. The threshold for a crystal to be included in the cluster is approximately $E_T = 1GeV$.

1 Photon conversion method: converted photons are reconstructed by combining the information in the ECAL and the trackers. This method relies on the difference in the shape of the E_t/p_t distributions between the signal and the background.

2 Isolation method: relies on the difference in the shape of the ISO distributions. For a photon signal, only pile-up, and detector noise may contribute to the ISO; the ISO falls off quickly around 5 GeV.

The weighted average of the differential cross sections measured with the two methods is reported as a function of E_T in four intervals of pseudorapidity: $|\eta| < 0.9$, $0.9 < |\eta| < 1.44$, $1.57 < |\eta| < 2.1$, and $2.1 < |\eta| < 2.5$.

4.6 Results on photon and diphoton production

In each paper, using the isolation technique the cross sections for different types of photon production were measured and results were compared to the LO, NLO and/or NNLO calculations.

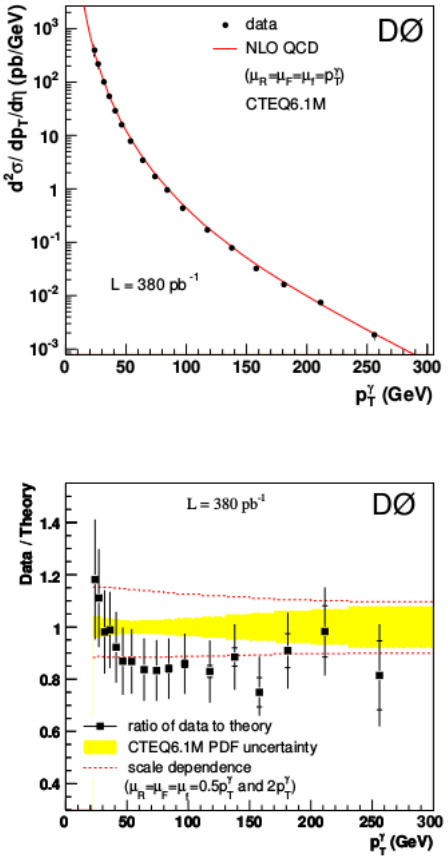

Figure 11: *Measured differential cross section for isolated photon production by D0 (top) and ratio of measured to predicted cross section by JETPHOX (bottom).*

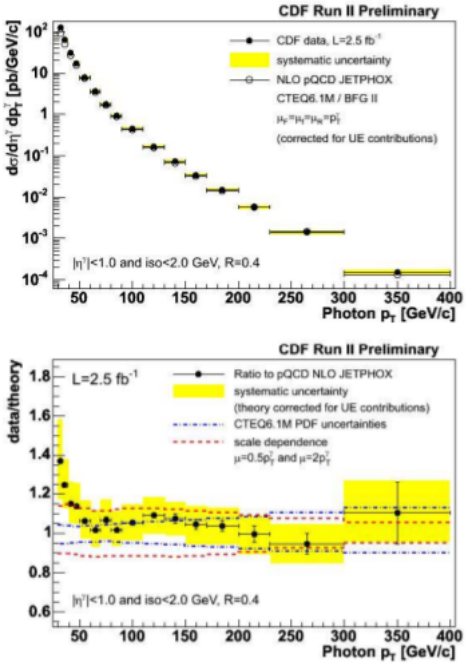

Figure 12: *Inclusive isolated photon cross section as a function of the photon transverse momentum measured by the CDF experiment (top) and theoretical predictions in NLO by JETPHOX (bottom).*

4.6.1 Inclusive photon cross section measurement at Tevatron for single photons

For the case of Tevatron measurements of prompt photon (direct photon) production in $p\bar{p}$ collisions were performed at a center of mass energy of $\sqrt{s} = 1.96TeV$, using a data sample corresponding to an integrated luminosity of $380pb^{-1}$(D0) and $2.5fb^{-1}$(CDF).

For D0, the measurements were performed in a range of $|\eta| < 0.9$ with $p_T > 23GeV$ in a cone of radius $\Delta R = 0.2$. For the isolation criteria, the transverse energy not associated to the photon in a cone of radius R=0.4 around a photon direction is required to be less than 0.10 times the energy of the photon,

$$E_T^{40} < 0.10 E_{EM}. \quad (8)$$

In the experiment CDF, the range is $|\eta| < 1.0$. Photon candidates are required to be isolated in the calorimeter with $E_T^{iso} < 2.0GeV$, where $E_T^{iso} = E_T^{40} - E_T^{\gamma}$.

For the D0 experiment in Figure. 11, the measured cross section is compared with the results from a NLO pQCD calculation. The results are consistent with theory within uncertainties. At low p_T there is a difference between theory and data which is difficult to interpret. Calculations that account for soft-gluon contributions are expected to provide better descriptions of the data at low p_T.

For CDF experiment in Figure. 12, theory (NLO pQCD predictions by JETPHOX) and data agree over the whole measured range except for p_T <40GeV where the data exhibits an excess. The systematic uncertainties in the cross section range from 10% to 15% dominated by photon purity determination at low p_T

4.6.2 Measurement of the differential cross section for isolated prompt photon at CMS

Photon candidates were identified with two methods for the measurement of the final cross section, one of them is show in Figure. (13).

The differential cross section in Figure. (14) obtained for the production of isolated prompt photon is in agreement with the NLO pQCD predictions within uncertainties, but a low E_T the prediction tend to be higher that the measured cross section.

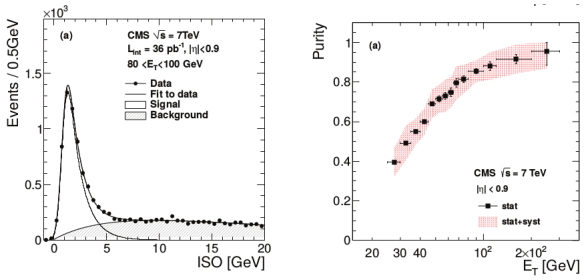

Figure 13: *The CMS distributions of ISO (left) for candidates with $E_T = 80 - 100GeV$. The fitted signal and background components are also shown. At the right, is the measured signal purity for ISO<5GeV with this method in the region $|\eta| < 0.9$.*

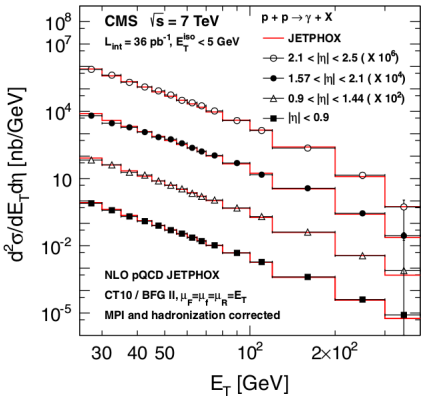

Figure 14: *Isolated prompt photon differential cross sections as a function of E_T in four pseudorapidity regions and predicions from JETPHOX, in CMS.*

4.6.3 Measurement of the cross section with two isolated photons at ATLAS

For ATLAS the isolated-diphoton production cross section in pp collisions was measured at 7TeV with $4.9 fb^{-1}$.

Also, the differential cross sections, as a function of the diphoton invariant mass, diphoton p_T and the azimuthal separation between the photons were measured.

The results were compared both to NLO and NNLO calculations (Figure. 15), obtained with parton-level MC generators.

The main difference is that at low p_T region the predictions fails to match the data, but this was expected because initial-state soft gluon radiation is divergent at NLO. For the higher order (NNLO) is still present an excess at low p_T .

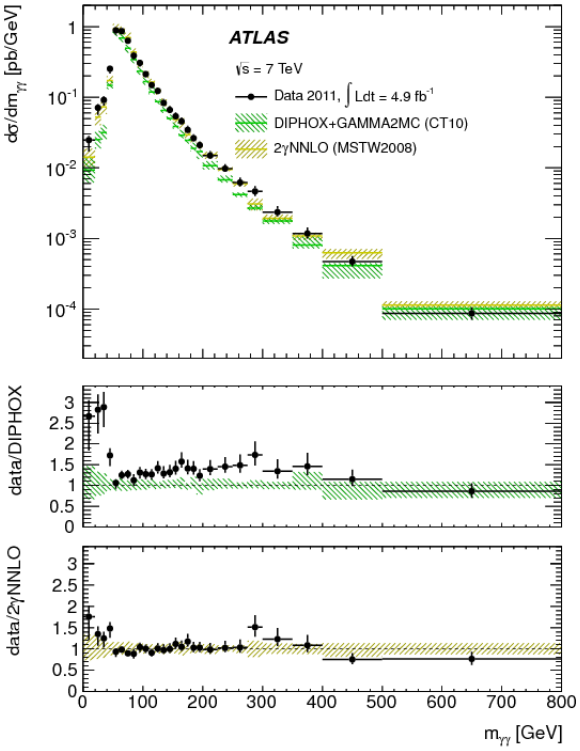

Figure 15: *Comparison between the experimental cross section as function of the transverse momentum and the predictions obtained for NNLO for $m_{,\gamma\gamma}$. The theoretical uncertainties include contributions from the limited size of the simulated sample. and from uncertainties on the parton distribution functions and on the hadronization.*

5 Conclusions

In experiments, isolation is defined with the calorimeter and/or tracking information within a cone of radius ΔR.

From the theoretical point of view photons are produced in two forms, direct and by a fragmentation process, so it is necessary to make an approximation where hadrons are allowed inside the isolation cone, at the border of which they can be as energetic as the photon itself, but are required to be softer the closer they are to the photon axis. Putting this into practice at experimental level is difficult because of the finite size of the granularity in calorimeters so the procedure can not go arbitrarily close.

Then, the proper matching between theoretical predictions and experiment results is not a trivial task.

The criteria for photon isolation vary in each experiment, but in all of them isolation is a key technique in photon analysis, due to background rejection and reduce the impact of the fragmentation contribution.

In the results of the different experiments there are systematic uncertainties in the cross section when comparing the data and the simulations, mostly at low p_T.

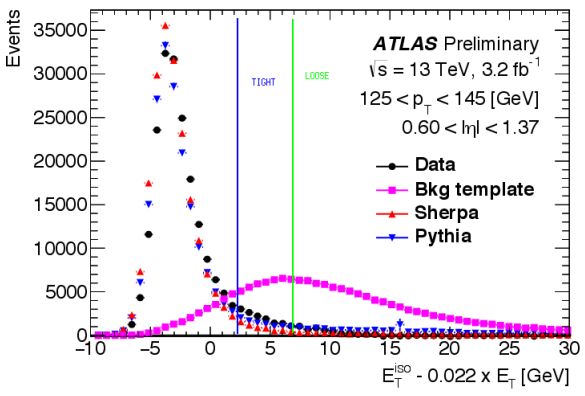

Figure 16: *Distributions of the calorimeter isolation variable for a photon candidates fulfilling the tight identification criteria for 125GeV< E_T <145 GeV and for the region 0.60< |η| <1.37. The tight (blue) and loose (green) line are indicated.*

5.1 Outlook

During the internship, the main task will be the characterization of isolation both for photons and fakes. Data and Monte Carlo simulations will be compared for and the agreement between them will be quantified, Figure. (16) shows the isolation distribution using 2015 data. Two simulations are shown with two different generators, each with advantages and disadvantages. In the case of PHYTIA, an incoherent sum of direct and fragmentation contributions is used, while SHERPA uses a matrix element that does not distinguish between direct and fragmentation process. SHERPA also implements a cut on true isolation at generation level.

The main deliveries are measurement of efficiency and purity for loose and tight cuts, with systematic uncertainties covering the data-MC agreement.

References

[1] M. Tripiana, "Medida de la sección eficaz de producción de fotones directos aislados en colisiones pp a $\sqrt{s} = 7$ TeV en el experimento ATLAS," CERN-THESIS-2012-022.

[2] G. Aad *et al.* [ATLAS Collaboration], "Observation of a new particle in the search for the Standard Model Higgs boson with the ATLAS detector at the LHC," Phys. Lett. B **716** (2012) 1

[3] G. Aad *et al.* [ATLAS Collaboration], "Measurement of Higgs boson production in the diphoton decay channel in pp collisions at center-of-mass energies of 7 and 8 TeV with the ATLAS detector," Phys. Rev. D **90** (2014) no.11, 112015

[4] G. Aad *et al.* [ATLAS Collaboration], "Measurement of isolated-photon pair production in *pp* collisions at $\sqrt{s} = 7$ TeV with the ATLAS detector," JHEP **1301** (2013) 086

[5] S. Chatrchyan *et al.* [CMS Collaboration], "Measurement of the Differential Cross Section for Isolated Prompt Photon Production in pp Collisions at 7 TeV," Phys. Rev. D **84** (2011) 052011

[6] A. Kumar [CDF and D0 Collaborations], "Prompt photon production at the Tevatron," FERMILAB-CONF-09-366-E.

[7] S. Frixione, "Isolated photons in perturbative QCD," Phys. Lett. B **429** (1998) 369

[8] L. Cieri, "Diphoton isolation studies," arXiv:1510.06873 [hep-ph].

[9] [ATLAS Collaboration], "Measurements of the photon identification efficiency with the ATLAS detector using 4.9 fb1 of pp collision data collected in 2011," ATLAS-CONF-2012-123.

[10] S. Laplace and J. B. de Vivie (2012). "Calorimetric isolation and pile-up, " ATLAS internal note.

[11] The ATLAS collaboration, "Search for resonances decaying to photon pairs in 3.2 fb^{-1} of *pp* collisions at $\sqrt{s} = 13$ TeV with the ATLAS detector," ATLAS-CONF-2015-081.

[12] The ATLAS collaboration, "Search for new phenomena in events with missing transverse momentum and a Higgs boson decaying to two photons in p p collisions at $\sqrt{s} = 13$ TeV with the ATLAS detector," ATLAS-CONF-2016-011.

[13] The ATLAS collaboration, ATLAS-CONF-2016-018.